Materials Research Proceedings 28 (2023) 761-770 https://doi.org/10.21741/9781644902479-83

A stress-based proposal for wrinkling criterion of clamped surfaces

BORBÉLY Richárd[1,a], KÖLÜS Martin L.[1,b] and BÉRES Gábor J.[1,c] *

[1]John von Neumann University, GAMF Faculty of Engineering and Computer Science, Izsáki road 10. 6000, Kecskemét, Hungary

[a]borbely.richard@gmaf.uni-neumann.hu, [b]kolus.martin@gamf.uni-neumann.hu, [c]beres.gabor@gamf.uni-neumann.hu

Keywords: Wrinkling Limit, Clamped Surfaces, Stress-Based Diagram

Abstract. This study presents a possible stress-based limit theory regarding the wrinkling occurrence of clamped surfaces. There are several theorems that describe the buckling and/or the wrinkling phenomenon in different forms and conditions, but a general description, which would represent the limit state of wrinkling in sheet metal forming still does not exist according to the authors knowledge. This could be particularly important for the finite element simulations that are mostly used for process minoring purposes. However, some software work with body elements is suitable for the representation of wrinkles, users do not receive information about how close a process is to the wrinkling limit, or how it is affected by the input parameters. This is even less estimable if shell, or membrane elements are used in a finite element code. In this work, a purely analytical calculation for the wrinkling limit stress of clamped surfaces is carried out, i.e., when blank holder tool acts on the sheet. To take into consideration the effect of the normal pressure, Wang and Cao's proposal was used. After expressing the critical stress by its major and minor principal components using anisotropic yield criteria, a novel illustration method of the wrinkling limit has become available and is published in this article.

Introduction

During the manufacturing of complex sheet parts in the press shop, necking or facture and the geometrical defects (like wrinkling and springback) are the most frequent failure modes [1]. Necking or fracture and wrinkling take place during the forming process, however springback can be considered as a post-forming defect. Although the occurrence of necking and fracture are deeply studied and different limit theorems are already introduced with the aim of process monitoring, wrinkling is less researched. Or at least, an accepted wrinkling limit theory for general cases (e.g., when blank holder also works) is not yet available, with the use of which one can monitor how close a process is to the risk of wrinkling. In this study a proposal can be seen for the stress-based wrinkling limit determination of clamped surfaces, using the basis of Wang and Cao's theory [2,3].

Most of the studies that cover the limits of formability, where the failure of a component is considered under different stress conditions and then the material behavior is summarized into one diagram, are directed to the classical forming limit diagram (FLD). This tool is accepted for necking evaluation in general by the sheet forming society. The FLD indicates the limit of global formability from shearing up to biaxial failure [4,5], i.e., the failure risk in negative (compression) stress states is less discussed in detail. Nevertheless, remarkable improvements have been made in the past, both on the practical determination [6] and the theoretical description [7] of the FLD. To this article, the development of the stress-based forming limit diagram proposed by Stoughton and Zhu [8] has a special importance, which calculation method partially forms the basis of the stress components' calculations applied in this manuscript.

In the respect of compression generated failure modes, the wrinkling is particularly problematic on sheet workpieces that require aesthetic appearance. Besides, wrinkles formed in the first drawing step can cause unpleasant complications in a subsequent press forming operation, too.

Content from this work may be used under the terms of the Creative Commons Attribution 3.0 license. Any further distribution of this work must maintain attribution to the author(s) and the title of the work, journal citation and DOI. Published under license by Materials Research Forum LLC.

Some of the parameters affecting this phenomenon are the stress state, the initial work piece geometry and the blank holder force. The latter one was analytically described by Ju and Johnson in an energy-based model [9] and was later used for discussing the behavior of axisymmetric drawn parts by Agrawal et al. [10]. The biggest drawback of this model is that it only works for cylindrical geometry.

Wang and Cao's article [2] lighted up a different, but also energy-based theorem, in which they proposed the calculation of the deformation energy of a completely flat sheet and a buckled sheet to judge the critical wrinkling conditions. The main advantage of this model is that it does not depend directly on the geometry, thus it is useful to any component geometry. They defined both the critical wrinkling stress as well as the optimal blank holder pressure that need to eliminate wrinkling, using the equations of anisotropic plasticity, expanded for different stress states in [3].

It should be also noted that, although the definition of rupture is perhaps exact even now, the onset of wrinkling is still based on individual subjective judgement. It is therefore necessary to define a preliminary boundary condition that is considered as the criterion of wrinkling. For example, in Wang and Cao's work, the transition from semi-sinusoidal to completely sinusoidal characteristic of surface wrinkles was nominated to the analytical condition. However, Hutchinson and Neale [11] developed an exact, purely theoretical equation (not detailed here), which states that wrinkling occurs when the sum of the bending stress and the stress resultants from buckling and stretching is zero, it is still not yet implemented in practice.

In this study, a possible way for wrinkling risk calculation is presented to define a wrinkling limit diagram that can serve as an input boundary for the design of forming processes. We base our claims on previous experimental investigations and numerical simulations, which are only partially addressed here.

Description of the Wrinkling Behavior

The analytical calculation of wrinkling limit criterion was carried out based on the proposals of Wang and Cao [2,3]. In this methodology, the critical, equivalent wrinkling stress can be obtained by the strain energy difference of a perfectly flat sheet (E_0) and a buckled sheet (E_b), during a deformation process. If negative stress acts on the edge of the component, i.e., for example on the flange of a drawn workpiece, wrinkling can develop if the strain energy of buckling is the larger one. However, when blank holder is applied during a deep drawing process, the optimum of the external work of the blank holder (W) is exactly the same as the difference of the two mentioned energy terms:

$$W = E_0 - E_b \tag{1}$$

Assuming that the external work of the blank holder can be mathematically described in the knowledge of the normal force and the buckling deflection, as well as the normal force itself is a non-linear function of the buckled height (δ), the normal pressure can be expressed in the following form, according to [2]:

$$p = \frac{3(E_0 - E_b)}{4\delta L w} \tag{2}$$

This is the case of a simplified, rectangular flat blank, which has L length, w width and s thickness (see Fig. 1). Applying the deduction of the energy terms based on [2,3], in which Swift hardening law [12] and Hill48 anisotropic plastic potential [13] was used, each energy members can be obtained according to Eq. 3 and Eq. 4.

$$E_0 = \frac{1}{w} \iint \bar{\sigma}\, d\bar{\varepsilon}\, dV = \frac{KLs}{n+1} (\varepsilon_0 + c_1 \varepsilon_{1_0})^{n+1} \tag{3}$$

$$E_b = \frac{2Ks}{n+1}\left[\frac{c_2 s}{2} + (\varepsilon_0 + c_3)\left(\frac{1}{m^2\delta} + \frac{s}{2}\right)\right]^{n+1} \cdot \left[\frac{1}{m^2\delta} + \frac{s}{2}\right]^{-n} \cdot tan^{-1}(m\delta) \quad (4)$$

In these functions, K, ε_0 and n refer to the constants of the Swift hardening law, while c_1, c_2 and c_3 are material parameters considering the plastic anisotropy and the stress state. The frequency of the wave mode is given by m.

With combining Eq. 1-4, the optimal blank holder pressure can be obtained by a purely analytical formula, which contains practically understandable material parameters as well as the u_t edge displacement and the L length of the blank:

$$p = \frac{3Ks}{4(n+1)\delta}\left\{\left[\varepsilon_0 + c_1 ln\left(1 - \frac{2u_t}{L}\right)\right]^{n+1} - \frac{2}{L}\left[\frac{c_2 s}{2} + (\varepsilon_0 + c_3)\cdot\left(\frac{1}{m^2\delta} + \frac{s}{2}\right)\right]^{n+1} \cdot \left[\frac{1}{m^2\delta} + \frac{s}{2}\right]^{-n} \cdot tan^{-1}(m\delta)\right\} \quad (5)$$

It means that the critical edge displacement (or the critical, normalized edge displacement u_{tcr}/L) for a given component length has to be known to obtain the critical normal pressure, which needs to eliminate wrinkling. Wang and Cao defined this critical value at the transition point, where half sinusoid wave form changes to a complete sinusoid wave form. With performing the above analysis (Eq. 1-5) by continuously changing L lengths (L_1, L_2, ..., L_i), intersecting curves will be output, at which the transition points will determine the edge displacement dependent function of the critical normal pressure:

$$p_1\left(L_1, \frac{u_{tcr}}{L}\right) - p_2\left(L_2, \frac{u_{tcr}}{L}\right) = 0 \quad (6)$$

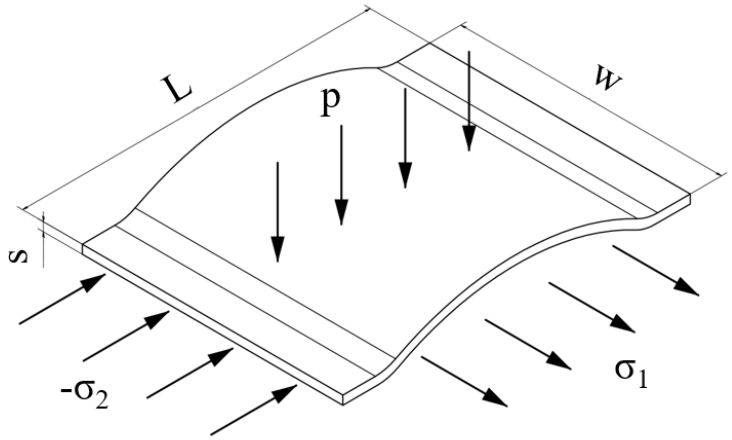

Fig. 1. A simplified, rectangular buckled sheet, affected by tension and compression stresses (the ut edge displacement is interpreted along the L direction).

Assuming that the equivalent plastic strain is direct function of the edge displacement and the stress state, it can be expressed from the associated flow rule that belongs to the Hill48 yield criterion, i.e.,

$$\varepsilon^{pl} = c_1 \cdot \ln\left(1 - \frac{2u_{tcr}}{L}\right) \quad (7)$$

In Eq. 7, c_1 parameter follows from the anisotropic criterion of yielding and embodies the effect of the stress state (α), too.

$$c_1 = \sqrt{\frac{1+r}{1+2r} \cdot \left(1 + \frac{r(1+\alpha)^2 + (\alpha+\alpha r-r)^2}{(1+r-\alpha r)^2}\right)} \tag{8}$$

The stress ratio is calculated as the ratio of the minor and the major principal stresses:

$$\alpha = -\frac{\sigma_2}{\sigma_1} \tag{9}$$

Now, the critical wrinkling stress can be considered as the equivalent stress, and it can be given in the function of the normal pressure. This fact also means that the critical pressure needs to eliminate wrinkling became known for any equivalent stress values that may be experienced in a deformable workpiece.

$$\sigma_{cr} = K\sqrt{\frac{1+r}{1+\alpha^2+r(1-\alpha)^2}}\left[\varepsilon_0 + c_1 \cdot ln\left(1 - \frac{2u_{tcr}}{L}\right)\right]^n \tag{10}$$

Proposal for the Wrinkling Limit Stress Diagram

For a given material, the hardening parameters (K, ε_0, n) and the average anisotropy coefficient (r) are constants in Eq. (10). Therefore, the slope of the σ_{cr}-p_{cr} curve only depends on the stress state. Fig. 2 shows an example for the calculated σ_{cr}-p_{cr} values of DC04 steel sheet, in which diagrams the equivalent stress is the same but the α stress ratio changes from -1/0.01 up to -1/1.0. The applied material parameters (K, ε_0, n and r) are listed slightly below in Table 1.

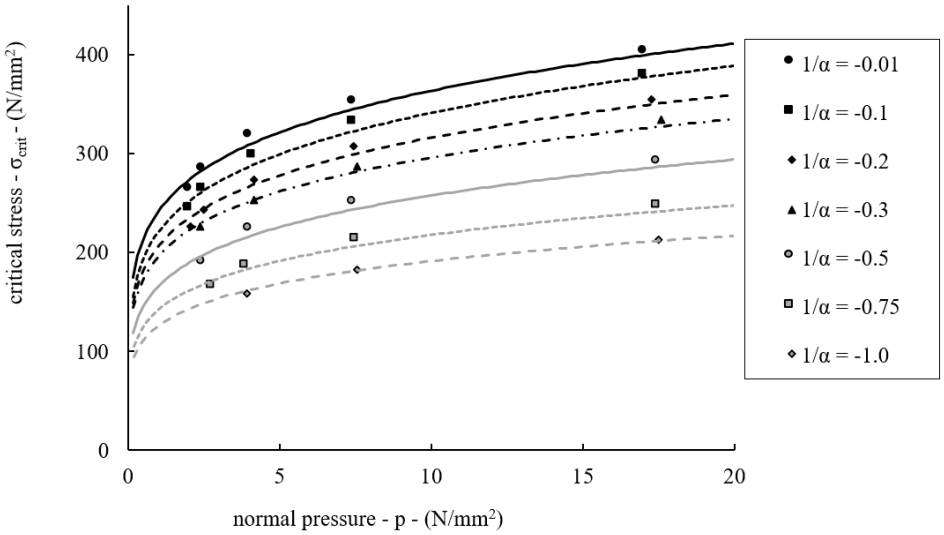

Fig. 2. The critical stress – critical pressure functions for different stress ratios.

Now it can be observed that α = -1/0.01 belongs to the nearly pure compression (the denominator cannot be zero) that exists on the outer sheet edge. With α = -1/1.00, the tension stress component is the same than the compression stress. At the surrounding regions of the inner edge of a drawn part, α = -1/0.20…+1/2.00 are typical values according to finite element simulations.

Considering the above phenomenon, the critical stress can therefore be determined for any blank holder pressure and for any stress ratio. Since the stress ratio is known for all coordinate points of a real workpiece in a finite element simulation, the risk of wrinkling can now be expressed as the function of the location coordinate. This does not only mean that the process monitoring can be achieved after implementing the curves of Fig. 2 into a finite element code (which is very time

consuming and complicated), but a clear and well-understandable limit diagram can also be created similar to the FLD. To do this, first, the stress ratio dependent relationship between the critical stress and the normal pressure should be determined analytically. Based on our experiences, it can be solved by simple power laws (Eq. 11), since the normal pressure is directly dependent on the amount of the plastic strain (see Eq. 3 – 5).

$$\sigma_{crit}(\alpha) = \gamma \cdot p^{\zeta} \tag{11}$$

In Eq. 11, the stress state dependent critical wrinkling stress is only expressed by two parameters. This model (continuous lines in Fig. 2) has relatively good agreement with the calculated points (dots in Fig. 2) in the practical range of the blank holder pressure. The regression coefficients of the power law curves are about $R^2 = 0.984…0.994$ for the different stress states.

Knowing the critical stress and the stress ratio, the associated, principal stress components can be calculated using an arbitrary yield criterion. Here we assume plain stress state, since the binder pressure is close to zero in practice ($\sim 2 \ldots 8\ \frac{N}{mm^2}$), thus it is much smaller than the tension (σ_1) and much higher than the compression ($-\sigma_2$) stresses (only exception is the outer edge where $\sigma_1 \approx 0$). Because Wang and Cao used the Hill48 quadratic yield function during the derivations of the energy terms, it is obvious to use it now, too. Although, there is not much difference in using other yield function, for example Yld89, as we shall see later.

Hill derived his suggestion for the yielding of anisotropic sheet metals on the basis of the von Mises yield criterion [1]. If the anisotropy axes coincide with the principal axes, the proposed model in plane stress state can be expressed in the following form:

$$2f(\boldsymbol{\sigma}) = H(\sigma_2 - \sigma_1)^2 + G\sigma_1^2 + F\sigma_2^2 = 1 \tag{12}$$

The relationship between the yield constants and the plastic strain ratios can be obtained by using the associated flow rule,

$$\frac{H}{G} = r_0;\ \frac{H}{F} = r_{90} \tag{13}$$

The yielding point at uniaxial loading ($\bar{\sigma} = \sigma_1\ and\ \sigma_2 = 0$) can be taken into account as

$$2f(\boldsymbol{\sigma}) = H\left(1 + \frac{1}{r_0}\right)\bar{\sigma}^2 \tag{14}$$

and hence the yield criterion can be defined through the plastic strain ratios:

$$\bar{\sigma}^2(r_0 + 1) = r_0(\sigma_2 - \sigma_1)^2 + \sigma_1^2 + \frac{r_0}{r_{90}}\sigma_2^2 \tag{15}$$

After some rearrangement and introducing α, we get

$$\bar{\sigma} = \sigma_1\sqrt{\left\{1 + \alpha^2\left[\frac{r_0(1+r_{90})}{r_{90}(1+r_0)}\right] - 2\alpha\frac{r_0}{1+r_0}\right\}} \tag{16}$$

Finally, the minor principal stress can be obtained by Eq. 9.

In the case of the Yld89 yield criterion, the determination of the principal stress components is originated from the equation of

$$f(\boldsymbol{\sigma}) = a|K_1 + K_2|^M + a|K_1 - K_2|^M + c|2K_2|^M = 2\bar{\sigma}^M \tag{17}$$

in which

$$K_1 = \frac{\sigma_1 + h\sigma_2}{2} \tag{18}$$

$$K_2 = \sqrt{\left(\frac{\sigma_1 - h\sigma_2}{2}\right)^2 + p^2\sigma_{12}^2} \tag{19}$$

If the coordinate system coincides with the principal directions, the shear stress and hence $p^2\sigma_{12}^2$ can be neglected, and the terms in brackets are simplified as follows:

$$K_1 + K_2 = \sigma_1$$

$$K_1 - K_2 = h\sigma_2 \tag{20}$$

Incorporating Eq. 20 into Eq. 17, the Yld89 yield theory will reduce to

$$f(\boldsymbol{\sigma}) = a|\sigma_1|^M + a|h\sigma_2|^M + c|\sigma_1 - h\sigma_2|^M = 2\bar{\sigma}^M \tag{21}$$

and the relationship between the major principal stress and the equivalent stress can be expressed using the stress ratio (α) again:

$$\sigma_1 \left\{\frac{1}{2}[a + a|h\alpha|^M + c|1 - h\alpha|^M]\right\}^{\frac{1}{M}} = \bar{\sigma} \tag{22}$$

The constants *a*, *c* and *h* can be determined from the strain ratios [14], while the minor principal stress component can be calculated from Eq. 10 again.

As a result of the derivations detailed above, the wrinkling criterion can be edited in the stress space analytically, which, like the FLD, provides a transparent method for process monitoring. As an example, the results obtained by the principal stresses' calculations for both the Hill48 and the Yld89 criteria can be seen in Fig. 3.

To this figure, the mechanical parameters of the applied DC04 sheet were characterized by tensile tests, and the necessary values are summarized in Table 1. (The data acquisition is not detailed here.)

Table 1. applied material parameters.

	K	ε_0	n	r_0	r_{90}
DC04	578	0.017	0.220	1.823	2.380

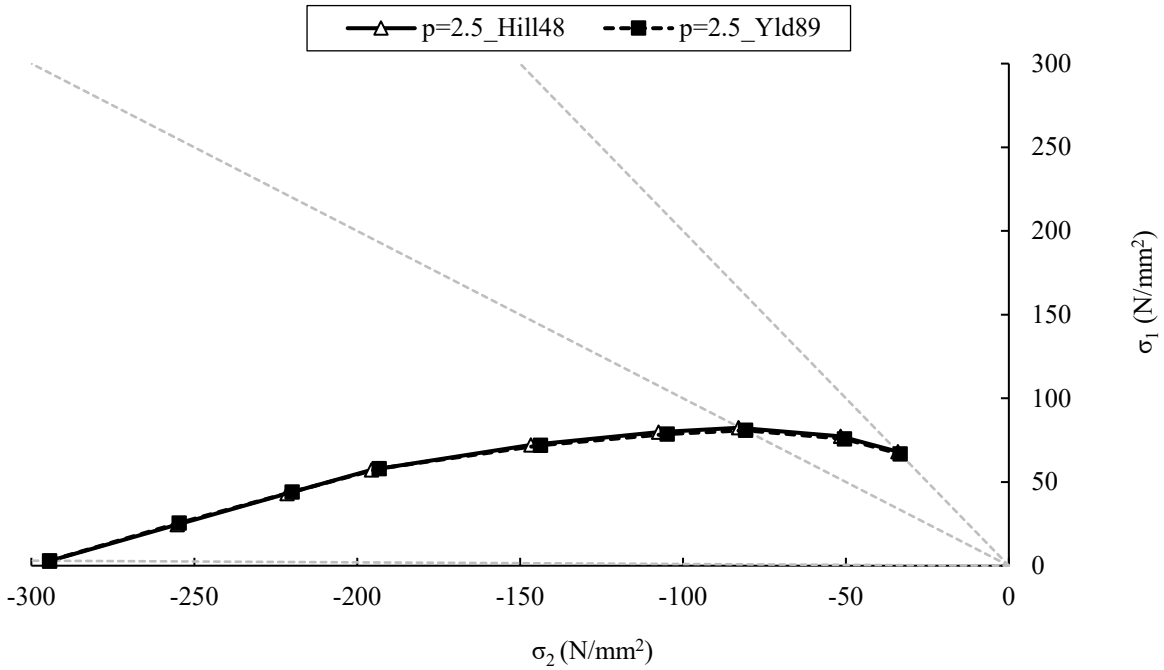

Fig. 3. Stress-based wrinkling limit curves calculated based on the Hill48 and the Yld89 yield criteria. The normal pressure value is 2.5 N/mm^2 for both cases.

It is worth mentioning that the calculated curves in Fig. 3 belong to $p = 2.5\ \frac{N}{mm^2}$ normal pressure. Since it was introduced that the wrinkling limit stress is the function of the blank holder pressure, the wrinkling limit diagram should be interpreted as a curve family, instead of one curve. With the shifting of the limit curve, both the effect of the stress state and the blank holder pressure can be visualized, as well as the limit values can be compared with numerical results. Fig. 4 shows the calculated limit curves of the DC04 sheet for three different blank holder pressures. In the graph, numerically obtained stress points from the outer edge of a drawn cup are also seen, just after the time step when wrinkles appear in the simulation at lower blank holder forces.

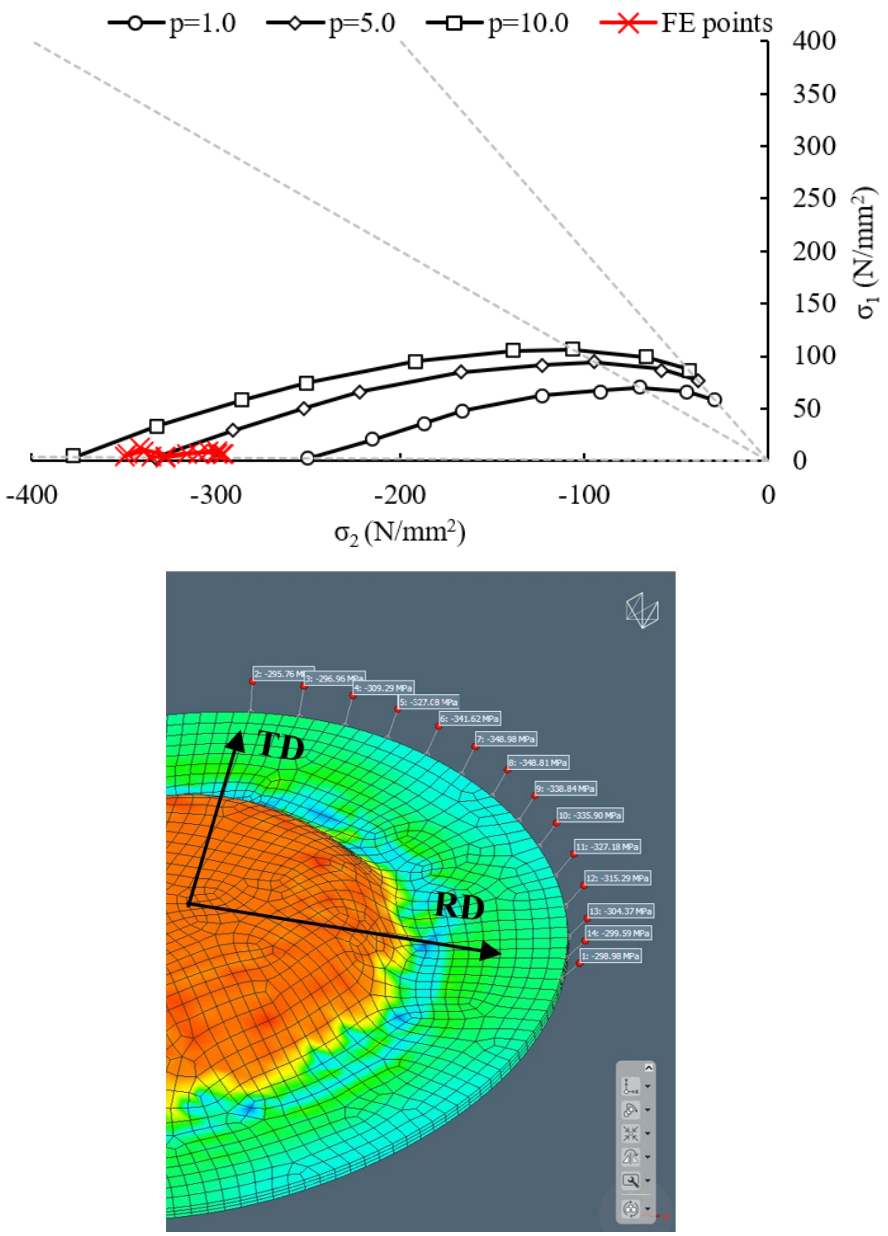

Fig. 4. Stress-based wrinkling limit curves for three different blank holder pressures and numerical points from a drawn part's flange. The pressure values are given in N/mm^2 in the graph, the applied blank holder pressure was 5 N/mm^2 in the simulation (no visible wrinkles).

The simulation was carried out in Simufact Forming 2021.1 software. The input material parameters are listed in Table 1, next to which Coulomb friction coefficient was used with the value of 0.12 on the die side and 0.20 on the punch side. The initial element size was 1.4 mm, and the sheet was discretized to three layers in the thickness direction that resulted in a total number of 6696 sheet mesh elements for a diameter Ø66 mm initial blank with 1 mm sheet thickness. The simulation results' validation was done by cup drawing tests supported by digital imagine correlation system, but a detailed insight to the measurements is not possible due to the limited content of the paper. The geometrical data of the tests are following. Punch diameter and radius: Ø33.0 mm and 5 mm; die diameter and radius: Ø35.4 mm and 5 mm (1.2 mm clearance). The applied blank holder pressure for the simulation results of Fig. 4 was 5 N/mm^2.

Consequently, it can be observed that the numerically obtained points form the outer perimeter of the flange are far above the limit curve of 1 N/mm^2 blank holder pressure, thus wrinkling is expected next to this value. At the same time, the stress points more or less fall below the limit curve of 5 N/mm^2, and wrinkles exist neither in the simulation, nor in the practice with this setting. Naturally, this analysis can be performed for any location point of a drawn part, although above α = 1/1.0 stress ratio, we do not think it make sense in terms of wrinkling.

It is also visible that the critical stress seems to be reached earlier at the inner region of the flange, since the decrease of the stress ratio causes the decrease of the compression stress, too. In this way authors recognize that this may lead to controversy and are currently working on the possible development of the theory.

Summary

With the calculation and then the allocation of the critical equivalent stress that causes wrinkling at a given blank holder pressure as indicated in this article, an easy-to-understand diagram was edited in the major and minor stresses' coordinate system. This diagram is logically consistent with the forming limit curve (either strain-, or stress-based), since it is also stress state dependent, but takes into consideration the blank holder pressure, too. Despite the simplifications during the calculations, the results that show the wrinkling risk at any specimen locations are comparable to the practical blank holder values. In addition, applying this criterion in a finite element code, the process monitoring from the perspective of wrinkling could become possible.

References

[1] D. Banabic, H.J. Bunge, K. Pöhlandt, A.E. Tekkaya, Formability of Metallic Materials, Springer-Verlag Berlin Heidelberg, 2000.

[2] X. Wang, J. Cao, An Analytical Prediction of Flange Wrinkling in Sheet Metal Forming, J. Manuf. Process. 2 (2000) 100-107. https://doi.org/10.1016/S1526-6125(00)70017-X

[3] J. Cao, X. Wang, An analytical model for plate wrinkling under tri-axial loading and its application, Int. J. Mech. Sci. 42 (2000) 617-633. https://doi.org/10.1016/S0020-7403(98)00138-6

[4] S. Keeler, W.A. Backofen, Trans. ASM 56 (1963) 25-48.

[5] G.M. Goodwin: Society of Automotive Engineers No. 680093 (1968) 380-387.

[6] M. Merklein, A. Kuppert, M. Geiger, Time dependent determination of forming limit diagrams, CIRP Annals – Manuf. Technol. 59 (2010) 295–298. https://doi.org/10.1016/j.cirp.2010.03.001

[7] D. Banabic, F. Barlat, O, Cazacu, T. Kuwabara, Advances in anisotropy and formability, Int. J. Mater. Form. 3 (2010) 165-189. https://doi.org/10.1007/s12289-010-0992-9

[8] T.B. Stoughton, X. Zhu, Review of theoretical models oft he strain-based FLD and their relevance to the stress-based FLD, Int. J. Plast. 20 (2004) 1463-1486. https://doi.org/10.1016/j.ijplas.2003.11.004

[9] T.X. Yu, W. Johnson, The buckling of annular plates in relation to the deep-drawing process, Int. J. Mech. Sci. 24, (1982) 175-188. https://doi.org/10.1016/0020-7403(82)90036-4

[10] A. Agrawal, N.V. Reddy, P.M. Dixit, Determination of optimum process parameters for wrinkle free products in deep drawing process, J. Mater. Process. Technol. 191 (2007) 51–54. http://doi.org/10.1016/j.jmatprotec.2007.03.050

[11] J.W. Hutchinson, K.W. Neale, Proceedings of Int. Symp. on Plastic Instability, Paris, France (1985) 1841–1914.

[12] H.W. Swift, Plastic instability under plane stress, J. Mech. Phys. Solid. 1 (1952) 1-18. https://doi.org/10.1016/0022-5096(52)90002-1

[13] R. Hill, A theory of the yielding and plastic flow of anisotropic metals, The hydrodynamics of non-Newtonian fluids I, Proceedings of the Royal Society of London. Series A, Mathematical and Physical Sciences 193 (1948) 281-297.
[14] F. Barlat, J. Lian, Plastic behavior and stretchability of sheet metals. Part I: A yield function for orthotropic sheets under plane stress conditions, Int. J. Plast. 5 (1989) 51-66. https://doi.org/10.1016/0749-6419(89)90019-3